Associated production of a *Z* boson and a single heavy-quark jet

J. Campbell,[1] R. K. Ellis,[2] F. Maltoni,[3,*] and S. Willenbrock[4,5]

[1]*High Energy Physics Division, Argonne National Laboratory, Argonne, Illinois 60439, USA*

[2]*Theoretical Physics Department, Fermi National Accelerator Laboratory, P. O. Box 500, Batavia, Illinois 60510, USA*

[3]*Centro Studi e Ricerche "Enrico Fermi," via Panisperna 89/A, 00184 Rome, Italy*

[4]*Department of Physics, University of Illinois at Urbana-Champaign, 1110 West Green Street, Urbana, Illinois 61801, USA*

[5]*Kavli Institute for Theoretical Physics, University of California, Santa Barbara, California 93106, USA*

The leading-order process for the production of a *Z* boson and a heavy-quark jet at hadron colliders is $gQ \to ZQ$ ($Q = c, b$). We calculate this cross section at next-to-leading order at the Fermilab Tevatron and the CERN LHC, and compare it with other sources of ZQ events. This process is a background to new physics, and can be used to measure the heavy-quark distribution function.

I. INTRODUCTION

Many signals for new physics at hadron colliders involve electroweak gauge bosons ($W^\pm, Z, \gamma$) and jets containing heavy quarks (c, b). The prime example is $W + 4$ jets, with one or more jets containing a *b* tag, which led to the discovery of the top quark [1–3]. Other examples include signals for the Higgs boson and the superpartners of the known particles [4,5]. It is therefore crucial to understand the standard-model background from the production of electroweak bosons and heavy-quark jets with good accuracy.

The simplest processes of this type are the production of a single electroweak gauge boson and one heavy-quark jet. In the case of the *W* boson, the leading-order process is $gs \to W^- c$ [6], which has been calculated at next-to-leading order (with m_c nonzero) [7]. For a photon, the leading-order process is $gQ \to \gamma Q$ ($Q = c, b$), which has also been calculated at next-to-leading order (with $m_Q = 0$) [8,9]. In this paper we consider the analogous leading-order process for the *Z* boson, $gQ \to ZQ$, shown in Fig. 1, which we calculate at next-to-leading order (with $m_Q = 0$).

An alternative calculational scheme is to regard $gg \to ZQ\bar{Q}$ as the leading-order process (with m_Q nonzero), and to allow one heavy quark to be emitted collinear to the beam, yielding a ZQ final state. This approach has two drawbacks. First, the expansion parameter of this calculation is $\alpha_S \ln(M_Z / m_Q)$ rather than α_S, so perturbation theory is less convergent. Using a heavy-quark distribution function sums these collinear logarithms to all orders, resulting in a perturbative expansion in α_S and $1/\ln(M_Z / m_Q)$ [10–12]. Second, it is much more difficult to obtain the next-to-leading-order correction to $gg \to ZQ\bar{Q}$ than to $gQ \to ZQ$, both because there is one more particle in the final state, and because the heavy-quark mass must be maintained in the calculation of $gg \to ZQ\bar{Q}$ to regulate the collinear region (one may set $m_Q = 0$ in $gQ \to ZQ$, provided that the heavy-quark transverse momentum is much larger than its mass). At present,

$gg \to ZQ\bar{Q}$ is known at next-to-leading order only for $m_Q = 0$ [13–15]. In contrast, the next-to-leading-order calculation of $gQ \to ZQ$ (with $m_Q = 0$) that we perform in this paper is sufficiently straightforward that the next-to-next-to-leading-order calculation may be available in the foreseeable future [16].

The process $gQ \to ZQ$ is a background to $gb \to hb$, where the *Z* boson and the Higgs boson decay to the same final state ($b\bar{b}$, $\tau^+ \tau^-$, or $\mu^+ \mu^-$) [17–19]. In addition, $gQ \to ZQ$ could potentially be used to measure the *Q* distribution function. The *b* distribution function is needed for the above-mentioned Higgs boson production process as well as for inclusive Higgs boson production, $b\bar{b} \to h$ [20–22]. It is also needed for the single-top quark production processes $qb \to q't$ [12,23] and $gb \to W^-t$ [24,25], and the charged-Higgs boson production process $gb \to H^-t$ [26–28]. The process $gQ \to \gamma Q$ is much more sensitive to the charm distribution function than to that of bottom quark, due to the greater electric charge of the charm quark [30,31].

At present, the *b* distribution function is derived perturbatively from the gluon distribution function [10,11,29] and there is no direct measurement of it. The *c* distribution function is similarly derived from the gluon distribution function, and it agrees well with direct measurements. Thus we expect the same to be true of the *b* distribution function. The uncertainty in the *b* distribution function derives from the uncertainty in the gluon distribution function.

Another source of ZQ events is $q\bar{q} \to ZQ\bar{Q}$, shown in Fig. 2, where either one *Q* is missed, or the two *Q*'s coalesce into a single jet. We show that this process is much more significant at the Fermilab Tevatron than at the CERN Large Hadron Collider (LHC), since light-quark distribution functions are relatively more important at large values of Bjorken *x*.
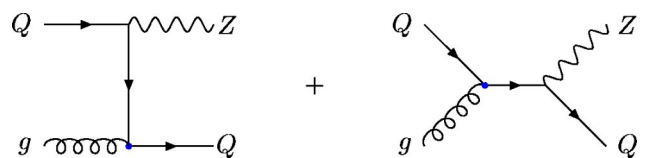

FIG. 1. Associated production of a *Z* boson and a single high-p_T heavy quark ($Q = c, b$).

————
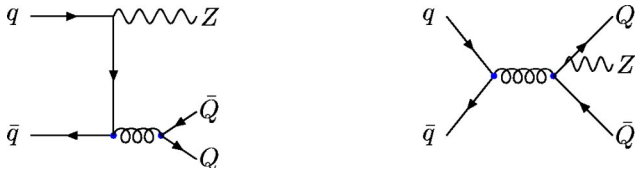*Mailing address: Dipartimento di Fisica, Terza Università di Roma, via della Vasca Navale 84, 00146 Rome, Italy.

FIG. 2. Representative Feynman diagrams for $q\bar{q}\to ZQ\bar{Q}$. The Z boson may be radiated off (a) the initial-state quarks or (b) the final-state quarks.

This calculation is carried out at leading order with a non-zero Q mass.

In addition, we also calculate Zj production at next-to-leading order, where j denotes a light-quark or gluon jet, as shown in Fig. 3 [32–34]. Using a silicon vertex detector to tag heavy quarks, the probability that such a jet fakes a heavy-quark jet is around 1%. Taking this probability into account, we show that this source of fake ZQ events is comparable to genuine ZQ events at the Tevatron, but is relatively less important at the CERN LHC.

All of the above processes can also lead to final states with two jets, with varying numbers of heavy quarks. For completeness, we also calculate these cross sections (at leading order). When combined with the next-to-leading-order cross section for ZQ, one obtains the inclusive cross section for Z plus at least one heavy-quark jet (at next-to-leading order).

The next-to-leading-order calculations in this paper were performed with the Monte Carlo code MCFM [35]. The leading-order calculations were performed both with this code and with MADEVENT [36].

II. $gQ\to ZQ$ AT NLO

The next-to-leading-order (NLO) calculation of $gQ\to ZQ$ parallels our NLO calculation of $gb\to hb$ [19], and we refer the reader to that work for a detailed discussion of the calculational scheme. The contributing subprocesses are

$gQ\to ZQ$ (one loop)
$qQ\to ZQq$
$gQ\to ZQg$
$gg\to ZQ\bar{Q}$.

The subprocess $q\bar{q}\to ZQ\bar{Q}$ is considered separately in the following section, and is not regarded as a correction to $gQ\to ZQ$.

We work in the simplified ACOT scheme [10,11], which allows one to neglect the Q mass throughout. This is a good approximation, and simplifies the calculation. The error made by this approximation is proportional to $1/\ln(M_Z/m_Q)$ $\times m_Q^2/p_T^2$ [19]. We use the dipole-subtraction method [37] as

FIG. 3. Representative Feynman diagrams for Zj production via (a) $gq\to Zq$ and (b) $q\bar{q}\to Zg$.

formulated in Ref. [38] to isolate and subtract collinear divergences.

In our NLO calculation of $gQ\to ZQ$, we demand one and only one jet with transverse momentum $p_T>15$ GeV within a rapidity range $|\eta|<2$ at the Fermilab Tevatron. This jet must contain a heavy quark. At the CERN Large Hadron Collider (LHC), the heavy-quark jet must have p_T >15 GeV and $|\eta|<2.5$.

If two partons lie within a cone of radius $\Delta R<0.7$, we merge them into a single jet with four-momentum equal to the sum of the two partons' four-momenta. This is done before the cuts described above are applied to the jets. The NLO process $gg\to ZQ\bar{Q}$ yields two heavy quarks in the final state. If they are merged into a single jet, we record it as a double-heavy-quark jet. This is only about 1% of the ZQ cross section.

Similarly, the NLO process $QQ'\to QQ'Z$, and processes related by crossing, yield two heavy quarks in the final state. However, these processes amount to a correction of less than 1%, so we neglect them [19].

We list in the first column of Tables I and II the LO (in parentheses) and NLO cross sections for $gb\to Zb$ and $gc\to Zc$ at the Tevatron and the LHC. The Zc cross section exceeds that of Zb by 70% at the Tevatron and 35% at the LHC because the charm distribution function is larger than that of bottom. This is partially compensated by the fact that the Z has stronger coupling to bottom than to charm. The ratio of the Zb and Zc partonic cross sections is proportional to

$$\frac{V_b^2+A_b^2}{V_c^2+A_c^2}=\frac{1+\left(1-\dfrac{4}{3}\sin^2\theta_W\right)^2}{1+\left(1-\dfrac{8}{3}\sin^2\theta_W\right)^2}\approx 13/10.$$

More importantly, a silicon vertex detector (SVX) can tag a b jet with an efficiency around 60%, and a c jet with an efficiency of about 15%. Thus the majority of ZQ events tagged with an SVX come from Zb.

The NLO processes that contribute to ZQ also give rise to final states with more than one jet, and we list these cross sections in the remaining columns. These events are grouped in three classes. The second column, labeled $Z(Q\bar{Q})$, corresponds to events with a single jet that contains two heavy quarks. As mentioned earlier, this is only about 1% of the ZQ cross section. The third column, labeled ZQj, corresponds to events with two jets, one of which contains a heavy quark. This is about 1/5 of the ZQ cross section at the Tevatron, and about 1/2 at the LHC (for $p_T>15$ GeV). The fourth column, labeled $ZQ\bar{Q}$, corresponds to events with two jets, both of which contain heavy quarks. This is significantly less than ZQj. The $ZQ\bar{Q}$ events arise from the NLO process $gg\to ZQ\bar{Q}$ (as do the $Z(Q\bar{Q})$ events). The final column sums these various processes, to give the inclusive cross section for Z plus at least one heavy-quark jet at next-to-leading order.

TABLE I. Cross sections (pb) for Z-boson production in association with heavy-quark jets at the Tevatron ($\sqrt{s}=1.96$ TeV $p\bar{p}$). A jet lies in the range $p_T>15$ GeV and $|\eta|<2$. Two final-state partons are merged into a single jet if $R_{jj}<0.7$. No branching ratios or tagging efficiencies are included. The labels on the columns have the following meaning: $ZQ=$ exactly one jet, which contains a heavy quark; $Z(Q\bar{Q})=$ exactly one jet, which contains two heavy quarks; $ZQj=$ exactly two jets, one of which contains a heavy quark; $ZQ\bar{Q}$ $=$ exactly two jets, both of which contain a heavy quark. For the last set of processes, the labels mean: Zj $=$ exactly one jet, which does not contain a heavy quark; $Zjj=$ exactly two jets, neither of which contain a heavy quark. For ZQ and Zj, both the leading-order (in parentheses) and next-to-leading-order cross sections are given. The last column is the next-to-leading-order inclusive cross section, which is the sum of four previous columns. The CTEQ6M parton distribution functions are used throughout, except for the LO cross sections in parentheses, where CTEQ6L1 is used [29]. The factorization and renormalization scales are chosen as $\mu_F=\mu_R=M_Z$. The uncertainties are from the variation of the renormalization scale, the factorization scale, and the parton distribution functions, respectively.

Cross sections (pb)		Tevatron			
	ZQ	$Z(Q\bar{Q})$	ZQj	$ZQ\bar{Q}$	ZQ inclusive
$gb\to Zb$	(8.23) 10.4	0.169	2.19	0.631	$13.4\pm0.9\pm0.8\pm0.8$
$q\bar{q}\to Zb\bar{b}$	3.32	1.92		1.59	6.83
$gc\to Zc$	(11.3) 16.5	0.130	3.22	0.49	$20.3\,^{+1.8}_{-1.5}\pm0.1\,^{+1.3}_{-1.2}$
$q\bar{q}\to Zc\bar{c}$	5.66	6.45		1.70	13.8
	Zj			Zjj	Zj inclusive
$q\bar{q}\to Zg, gq\to Zq$	(876) 870			137	$1010\,^{+44}_{-40}\,^{+9}_{-2}\,^{+7}_{-12}$

We show in Figs. 4–7 the scale dependence of the inclusive cross section for Zb and Zc production at the Tevatron and the LHC at leading order (LO) and next-to-leading order (NLO). The dependence on the renormalization and factorization scales are shown separately. Both scale dependencies are reduced at NLO in comparison with LO. We use $\mu_R=M_Z$, $\mu_F=M_Z$ as our default value of the renormalization and factorization scales.

We also estimate the uncertainty in the NLO inclusive cross section. The first uncertainty is due to varying the renormalization scale between half and twice its default value of $\mu_R=M_Z$. The second uncertainty, obtained in the same manner, is due to the factorization scale. The third uncertainty is from the parton distribution functions [29]. There is also an additional uncertainty of 4% due to $\delta\alpha_S(M_Z)=0.002$ [39].

We show in Figs. 8 and 9 the transverse-momentum distributions of both the Z and the highest-p_T b jet at the Tevatron and the LHC. At leading order these distributions are identical, since the Z recoils against the b jet. At next-to-leading order the distributions for the inclusive cross section are slightly different, since the Z can recoil against two jets. The distributions for Zc production are qualitatively similar.

III. $q\bar{q}\to ZQ\bar{Q}$ AT LO

Another contribution to ZQ production comes from $q\bar{q}$ $\to ZQ\bar{Q}$ ($q=u,d,s$), shown in Fig. 2, where one Q is outside the coverage of the detector. The dominant contribution to the cross section comes from diagrams in which the Z is radiated from the initial-state quarks while the heavy quarks arise from gluon splitting, as shown in Fig. 2(a). We maintain the heavy-quark mass throughout the calculation in order to regulate the singularity that would arise from a gluon splitting to massless collinear quarks. Although the NLO cross section for this process with massless quarks is available [13–15], the cross section with massive quarks is known only at LO.

TABLE II. Same as Table I, except at the LHC ($\sqrt{s}=14$ TeV pp). A jet lies in the range $p_T>15$ GeV and $|\eta|<2.5$.

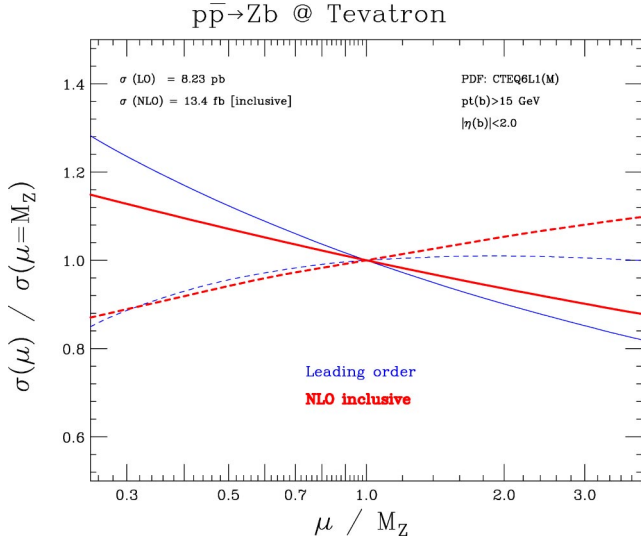| Cross sections (pb)		LHC			
	ZQ	$Z(Q\bar{Q})$	ZQj	$ZQ\bar{Q}$	ZQ inclusive
$gb\to Zb$	(826) 649	11.3	304	78.1	$1040\,^{+70}_{-60}\,^{+70}_{-100}\,^{+30}_{-50}$
$q\bar{q}\to Zb\bar{b}$	24.3	13.5		11.4	49.2
$gc\to Zc$	(989) 921	8.8	396	61.5	$1390\pm100\,^{+60}_{-70}\,^{+40}_{-80}$
$q\bar{q}\to Zc\bar{c}$	36.7	41.7		11.3	89.7
	Zj			Zjj	Zj inclusive
$q\bar{q}\to Zg, gq\to Zq$	(13500) 11600			4270	$15870\,^{+900}_{-600}\,^{+60}_{-300}\,^{+300}_{-500}$

FIG. 4. Cross section for $gb \to Zb$ at the Tevatron vs. the renormalization scale (solid curves) and factorization scale (dashed curves). The ratio of the cross section at scale μ to the cross section at scale $\mu = M_Z$ is plotted vs. the ratio of the scales. The next-to-leading-order (NLO) inclusive cross section (bold) is less sensitive to the scales than the leading-order (LO) cross section (regular).

The LO cross section for ZQ production via $q\bar{q} \to ZQ\bar{Q}$ is given in the first column of Tables I and II. At the Tevatron, the cross section is about $1/3$ of $gQ \to ZQ$. At the LHC, the contribution from $q\bar{q} \to ZQ\bar{Q}$ is relatively much less, only about $1/30$ of $gQ \to ZQ$. This reflects the fact that this process is initiated by a $q\bar{q}$ collision. At the Tevatron, where the typical values of Bjorken x are relatively large, the valence quark distribution functions are significant. In contrast, the typical values of x are relatively small at the LHC, so the valence quark distribution functions are less important.

The second column in Tables I and II lists the contribution from $q\bar{q} \to ZQ\bar{Q}$ when the Q and $\bar{Q}$ merge into a single jet. This is comparable in size to the contribution of this process
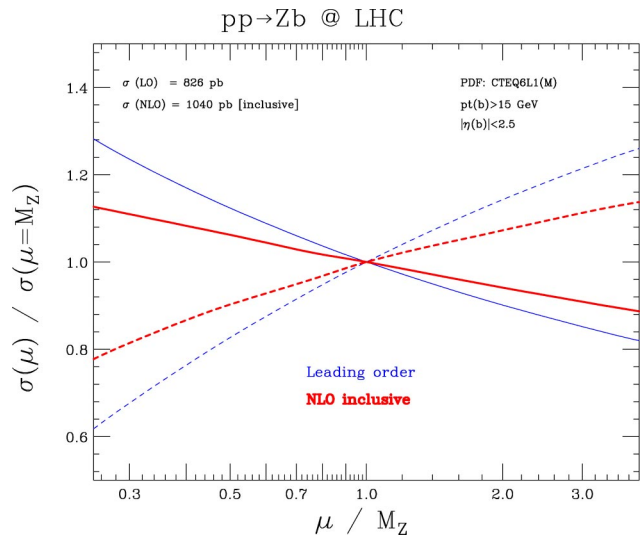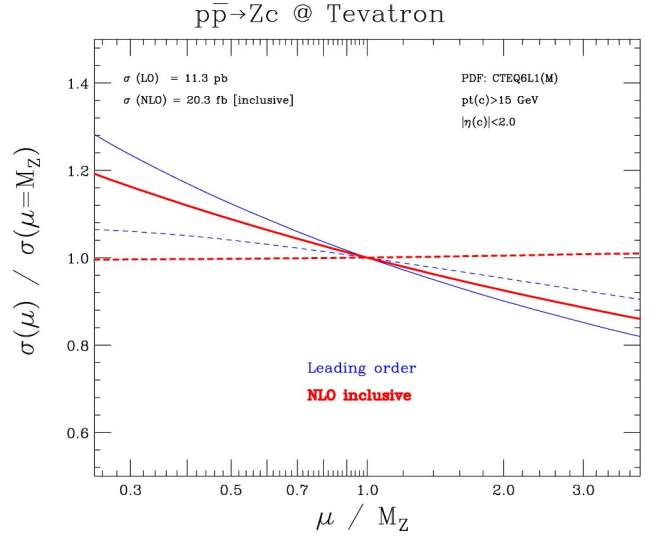

FIG. 6. Same as Fig. 4, but for Zc production.

to ZQ production. This is due to the aforementioned enhancement that arises when the heavy quarks are collinear. This process is the dominant source of events where the Z is accompanied by a single jet that contains two heavy quarks.

The last column gives the contribution of $q\bar{q} \to ZQ\bar{Q}$ when both jets are within the coverage of the detector. The $Zb\bar{b}$ cross section is about $1/2$ of the Zb cross section from this process at both machines, and the $Zc\bar{c}$ cross section is about $1/3$ of the Zc cross section. This is in contrast with the $gQ \to ZQ$ process, where the $ZQ\bar{Q}$ final state (that arises at NLO) is much less than ZQ.

IV. $q\bar{q} \to Zg$, $gq \to Zq$ AT NLO

A light-quark or gluon jet can fake a heavy-quark jet. With a silicon vertex detector, the mistagging rate is typically around 1%. Since the cross section for Zj production is much
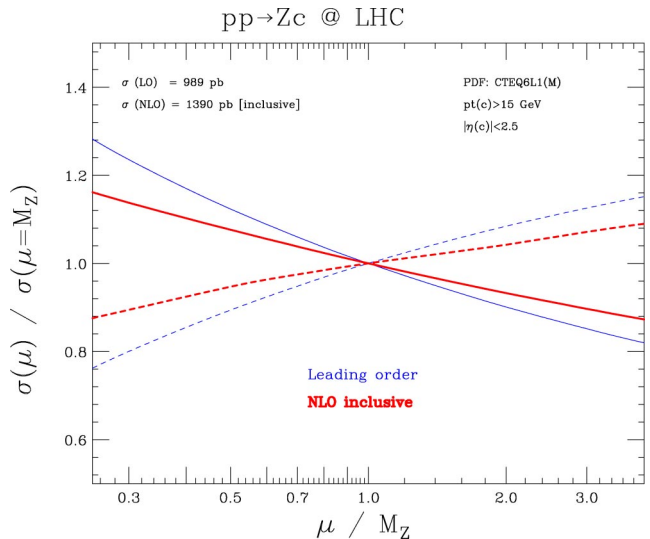

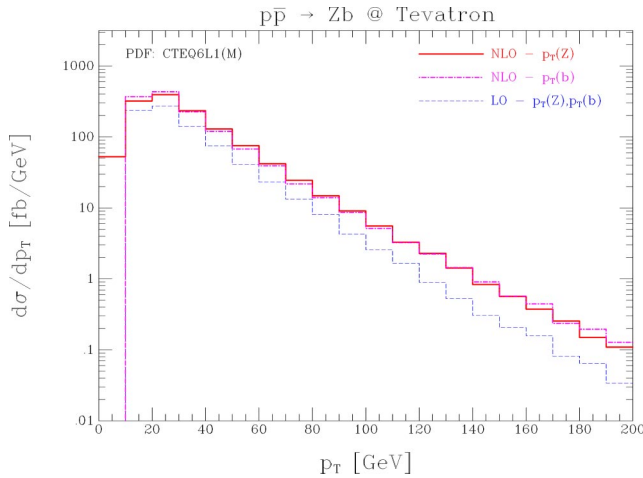FIG. 5. Same as Fig. 4, but at the LHC.

FIG. 7. Same as Fig. 6, but at the LHC.

FIG. 8. The transverse-momentum distribution of $gb \to Zb$ at the Tevatron. Qualitatively similar results are obtained for $gc \to Zc$. The LO curve is the p_T of either the Z or the b jet. At NLO, the distributions of both the Z and the highest-p_T b jet are shown for the inclusive cross section.

greater than that for ZQ, it is potentially a large source of fake ZQ events.

We list in Tables I and II the LO (in parentheses) and NLO cross sections for Zj production. The LO processes are $q\bar{q} \to Zg$ $(q = u,d,s,c,b)$ and $gq \to Zq$ $(q = u,d,s)$, as shown in Fig. 3. The NLO processes also contribute to the Zjj final state, and we list that cross section in the tables as well. The Zj cross section is almost two orders of magnitude greater than that of $gQ \to ZQ$ at the Tevatron. Taking into account the 1% mistagging rate, we see that Zj is a significant source of fake ZQ events at the Tevatron. In contrast, at the LHC the Zj cross section is not nearly as significant. Thus there will be relatively fewer mistagged events at the LHC. Qualitatively similar results are obtained for the ratio of Zjj to ZQj.
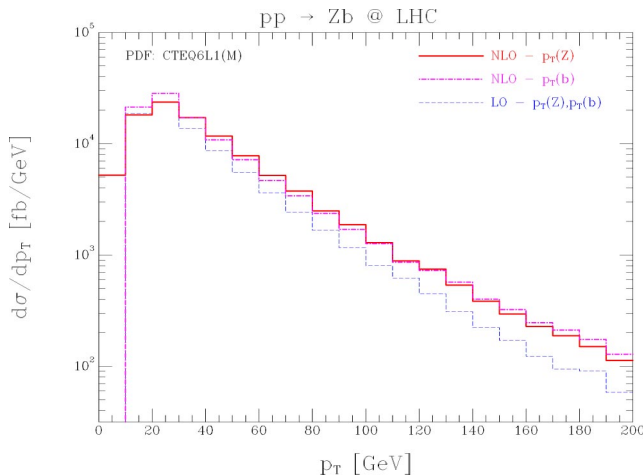

FIG. 9. Same as Fig. 8, but at the LHC.

V. CONCLUSIONS

The dominant contribution to Zb production is $gb \to Zb$. At the Tevatron, $q\bar{q} \to Zb\bar{b}$ also makes a significant contribution. Combining these two contributions, the total inclusive cross section for Zb production at the Tevatron is about 20 pb. Thus there are about 2000 inclusive Zb events produced within the coverage of the detector at the Tevatron for every 100 pb^{-1} of integrated luminosity delivered. The cleanest decay mode of the Z boson is to leptons ($\ell = e,\mu$), with a branching ratio of 6.7%. Including a b-tagging efficiency of 60% yields about 80 tagged ($Z \to \ell^+ \ell^-$)b events for every 100 pb^{-1}. There are slightly more tagged events when one accounts for the fact that some events contain two heavy quarks, either within the same jet or in separate jets. With data sets between 4000 and 8000 pb^{-1} expected in run II at the Tevatron, there will be between 3200 and 6400 tagged ($Z \to \ell^+ \ell^-$)b events.

At the LHC, the contribution from $q\bar{q} \to Zb\bar{b}$ is much less significant, so most of the cross section comes from $gb \to Zb$. The total inclusive cross section for Zb production is about 1090 pb, a factor of about 50 larger than at the Tevatron. Thus there will be an enormous number of Zb events at the LHC.

The total inclusive cross section for Zc production at the Tevatron is about 70% greater than that of Zb, while at the LHC, Zc is about 35% greater than Zb. However, the SVX tagging efficiency for charm is about 1/4 of the b-tagging efficiency, so there will be fewer tagged Zc events than tagged Zb events. In contrast, the number of γc events far outweighs the number of γb events at both machines, since charm has twice the electric charge of bottom and the charm distribution function is larger than that of bottom. Even taking the greater tagging efficiency of bottom into account, the number of tagged γc events is larger than the number of tagged γb events [30,31].

Zj events, where the jet is mistagged as a heavy quark, are a significant source of fake ZQ events at the Tevatron, but much less so at the LHC. Thus a larger fraction of the tagged ZQ events at the LHC will be from genuine heavy-quark production. For this reason, and also due to the relatively smaller contribution from $q\bar{q} \to ZQ\bar{Q}$, the LHC provides a cleaner environment for the extraction of the heavy-quark distribution functions via $gQ \to ZQ$.

In addition to the decay $Z \to \ell^+ \ell^-$, there will be many $Z \to \nu\bar{\nu}$ events ($BR = 20\%$), which will yield heavy-quark monojets. This will also yield dijet events with large missing transverse momentum, with one or both jets containing heavy quarks.

Regardless of the Z decay mode, the majority of $Z + 2$ jet events with a single heavy-quark tag at the LHC come from ZQj, not $ZQ\bar{Q}$. At the Tevatron, where $q\bar{q} \to ZQ\bar{Q}$ is relatively more important, the ZQj and $ZQ\bar{Q}$ final states are comparable in size.

ACKNOWLEDGMENTS

[1] CDF Collaboration, F. Abe *et al.*, Phys. Rev. Lett. **74**, 2626 (1995).

[2] D0 Collaboration, S. Abachi *et al.*, Phys. Rev. Lett. **74**, 2632 (1995).

[3] CDF Collaboration, D. Acosta *et al.*, Phys. Rev. D **65**, 052007 (2002).

[4] M. Carena and J. Lykken, "Physics at Run II: Supersymmetry/Higgs Workshop," FERMILAB-PUB-00-349, prepared for Physics at Run II: Workshop on Supersymmetry/Higgs: 1st General Meeting, Batavia, Illinois, 1998.

[5] ATLAS Collaboration, Technical Design Report, CERN-LHCC-99-15.

[6] U. Baur, F. Halzen, S. Keller, M.L. Mangano, and K. Riesselmann, Phys. Lett. B **318**, 544 (1993).

[7] W.T. Giele, S. Keller, and E. Laenen, Phys. Lett. B **372**, 141 (1996).

[8] E.L. Berger and L.E. Gordon, Phys. Rev. D **54**, 2279 (1996).

[9] B. Bailey, E.L. Berger, and L.E. Gordon, Phys. Rev. D **54**, 1896 (1996).

[10] M.A. Aivazis, J.C. Collins, F.I. Olness, and W.K. Tung, Phys. Rev. D **50**, 3102 (1994).

[11] J.C. Collins, Phys. Rev. D **58**, 094002 (1998).

[12] T. Stelzer, Z. Sullivan, and S. Willenbrock, Phys. Rev. D **56**, 5919 (1997).

[13] J.M. Campbell and R.K. Ellis, Phys. Rev. D **62**, 114012 (2000).

[14] J. Campbell and R.K. Ellis, Phys. Rev. D **65**, 113007 (2002).

[15] J. Campbell, R.K. Ellis, and D. Rainwater, Phys. Rev. D **68**, 094021 (2003).

[16] E.W.N. Glover, Nucl. Phys. B (Proc. Suppl.) **116**, 3 (2003).

[17] D. Choudhury, A. Datta, and S. Raychaudhuri, hep-ph/9809552.

[18] C.S. Huang and S.H. Zhu, Phys. Rev. D **60**, 075012 (1999).

[19] J. Campbell, R.K. Ellis, F. Maltoni, and S. Willenbrock, Phys. Rev. D **67**, 095002 (2003).

[20] D. Dicus, T. Stelzer, Z. Sullivan, and S. Willenbrock, Phys. Rev. D **59**, 094016 (1999).

[21] C. Balazs, H.J. He, and C.P. Yuan, Phys. Rev. D **60**, 114001 (1999).

[22] F. Maltoni, Z. Sullivan, and S. Willenbrock, Phys. Rev. D **67**, 093005 (2003).

[23] T. Stelzer, Z. Sullivan, and S. Willenbrock, Phys. Rev. D **58**, 094021 (1998).

[24] A.P. Heinson, A.S. Belyaev, and E.E. Boos, Phys. Rev. D **56**, 3114 (1997).

[25] S. Zhu, Phys. Lett. B **524**, 283 (2002); **537**, 351(E) (2002).

[26] V.D. Barger, R.J.N. Phillips, and D.P. Roy, Phys. Lett. B **324**, 236 (1994).

[27] S.h. Zhu, Phys. Rev. D **67**, 075006 (2003).

[28] T. Plehn, Phys. Rev. D **67**, 014018 (2003).

[29] J. Pumplin, D.R. Stump, J. Huston, H.L. Lai, P. Nadolsky, and W.K. Tung, J. High Energy Phys. **07**, 012 (2002).

[30] CDF Collaboration, F. Abe *et al.*, Phys. Rev. Lett. **83**, 3124 (1999).

[31] CDF Collaboration, T. Affolder *et al.*, Phys. Rev. D **65**, 052006 (2002).

[32] P.B. Arnold and M.H. Reno, Nucl. Phys. **B319**, 37 (1989); **B330**, 284(E) (1990).

[33] R.J. Gonsalves, J. Pawlowski, and C.F. Wai, Phys. Rev. D **40**, 2245 (1989).

[34] W.T. Giele, E.W. Glover, and D.A. Kosower, Nucl. Phys. **B403**, 633 (1993).

[35] QCD Tools Working Group Collaboration, R.K. Ellis *et al.*, hep-ph/0011122.

[36] F. Maltoni and T. Stelzer, J. High Energy Phys. **02**, 027 (2003).

[37] R.K. Ellis, D.A. Ross, and A.E. Terrano, Nucl. Phys. **B178**, 421 (1981).

[38] S. Catani and M.H. Seymour, Nucl. Phys. **B485**, 291 (1997); **B510**, 503(E) (1997).

[39] Particle Data Group, K. Hagiwara *et al.*, Phys. Rev. D **66**, 010001 (2002).